Nature of the Magnetic Interactions in Sr_3NiIrO_6

Turan Birol
Department of Physics and Astronomy, Rutgers University, Piscataway, New Jersey 08854, USA and
Department of Chemical Engineering and Materials Science,
University of Minnesota, Minneapolis, Minnesota 55455, USA

Kristjan Haule and David Vanderbilt
Department of Physics and Astronomy, Rutgers University, Piscataway, New Jersey 08854, USA
(Dated: May 11, 2018)

Iridates abound with interesting magnetic behaviours because of their strong spin-orbit coupling. Sr_3NiIrO_6 brings together the spin-orbital entanglement of the Ir^{4+} ion with a 3*d* Ni cation and a one-dimensional crystal structure. It has a ferrimagnetic ground state with a 55 T coercive field. We perform a theoretical study of the magnetic interactions in this compound, and elucidate the role of anisotropic symmetric exchange as the source of its strong magnetic anisotropy. Our first-principles calculations reproduce the magnon spectra of this compound and predict a signature in the cross sections that can differentiate the anisotropic exchange from single-ion anisotopy.

Oxides of 5*d* transition metals, especially iridates, are at the center of recent interest because of their strong spin-orbit coupling (SOC) [1, 2]. SOC gives rise to novel phenomena such as anisotropic pseudodipolar magnetic exchange interactions [3]. These interactions in turn lead to phases such as the quantum spin liquid in the Kitaev model, which might be realized in honeycomb iridates [4].

The magnetic behaviour of complex oxides with multiple inequivalent transition-metal cations can also be very rich, especially when the transition metals come from different rows of the periodic table. For example, the 3*d*-5*d* double perovskites are known to display incommensurate antiferromagnetism, multiferroicity, magnetoresistance, half-metallic ferrimagnetism, independent ordering of interpenetrating magnetic lattices, and very often high ordering temperatures [5–9]. Novel phenomena are still being discovered in these systems, as for example the recent demonstration of magnetic interactions in Ca_2CoOsO_6 and Ca_2NiOsO_6 that break the Goodenough-Kanamori-Anderson (GKA) rules [10].

Another structural family of compounds that contain two different transition-metal cations is that of the $A_3MM'O_6$ chain compounds with the K_4CdCl_6 crystal structure [11]. Many members of this family exhibit phenomena such as multiferroicity, unexpectedly strong magnetic anisotropy, colossal magnon gaps, superparamagnetic-like behaviour, and partially disordered antiferromagnetism [12–17]. Ferrimagnetic Sr_3NiIrO_6 [18], a member of this family, displays Ising-like magnetic anisotropy, a record-breaking magnetic coercive field [19], and a colossal spin wave gap [20, 21]. All of these are surprising observations because neither Ni^{2+} nor Ir^{4+} should have strong single-ion magnetic anisotropy (SIA).

In this work, we approach the magnetic interactions in Sr_3NiIrO_6 from first principles and elucidate the microscopic mechanism behind its magnetism. Our main result is that the interaction between nearest neighbor magnetic moments $\mathbf{M}_i$ is symmetric but radically anisotropic, i.e., it has the form $J_\parallel M_{i,z}M_{i+1,z} + J_\perp (M_{i,x}M_{i+1,x} + M_{i,y}M_{i+1,y})$ where $J_\parallel$ and $J_\perp$ have opposite signs. This anisotropic exchange induces strong Ising-like behaviour even in the absence of any SIA. Using this model with parameters fitted to first-principles calculations, we extract the magnon spectra and reproduce the qualitative aspects of the experimental observations of a small bandwidth and a colossal gap [20, 21]. We conclude by predicting a signature in the magnon-creation neutron-scattering cross section that can differentiate between the anisotropic exchange scenario and the commonly used isotropic exchange with strong SIA.

Sr_3NiIrO_6 has been previously studied theoretically by multiple authors, starting with Vajenine and Hoffmann's Hueckel calculations [22]. Zhang et al., using Density Functional Theory (DFT), underlined the importance of the SOC, and reported considerable orbital moments for both transition metals [23]. Sarkar et al. verified the presence of large orbital moments [24]. Ou and Wu pointed out the importance of SOC in altering the orbital configuration of Ir, and found that it is responsible for the intrachain ferrimagnetic order [25]. Most recently, Gordon et al. elucidated a connection between the magnetic exchange interactions and the Ising behaviour in Sr_3NiIrO_6 [26]. Our work goes beyond these first-principles calculations, and in addition to explaining the microscopic mechanism of the anisotropic exchange interaction in this 3*d*-5*d* system, bridges the gap between the first-principles calculations and experimental observations by calculating the magnetic interaction parameters from first principles and reproducing the experimentally observed magnon spectra.

The structure of Sr_3NiIrO_6 consists of parallel one-dimensional chains of alternating face-sharing NiO_6 and IrO_6 polyhedra as shown in Fig. 1(a) [11, 18]. There are two different energy scales for magnetic couplings along the *c* axis (intrachain) and in the *ab* plane (in-

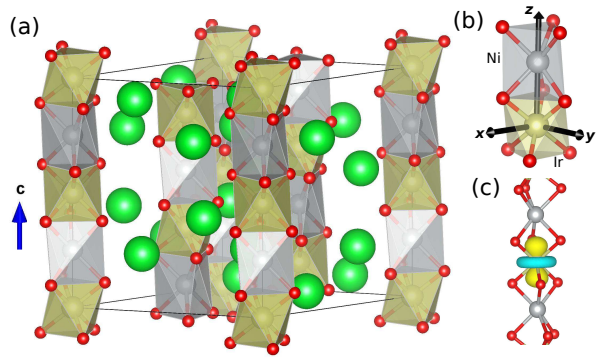

FIG. 1. (Color Online) (a) Crystal structure of Sr_3NiIrO_6 (b) The local axes used for the Ir ions. (c) The $|3z^2 - r^2\rangle$ orbital on an Ir ion.

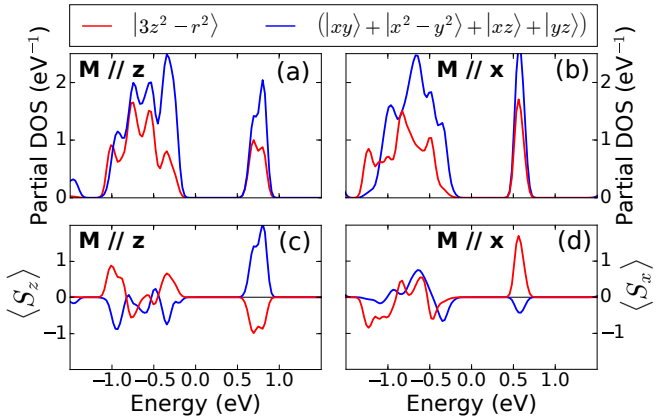

FIG. 2. (Color Online) (a) Densities of states of the Ir ion projected onto the d orbitals in the FiM state with magnetic moments along the z axis (magnetic ground state). (b) Same quantity as in (a), but in the FM state with magnetic moments along the x axis. (c) Energy resolved expectation value of the z component of spin, $\langle S_z\rangle$ for the d orbitals of the Ir ion in the FiM state with magnetic moments along the z axis. (d) Same quantity as in (c), but in the FM state with magnetic moments along the x axis.

terchain). Similarly, there are two temperature scales for magnetism. At T_2, intrachain magnetic order sets in. The temperature scale for the interchain magnetic order, T_1, is usually about an order of magnitude smaller than T_2. This is because there are no good superexchange paths that connect magnetic moments in different chains, but also because the chains form a frustrated triangular lattice. In Sr_3NiIrO_6, $T_2 = 75$ K, and the intrachain order is ferrimagnetic: both the Ni and Ir moments are aligned along the c axis (chain direction), but are antiparallel to each other [27]. The interchain order below $T_1 = 17$ K is still under debate: neutron data is consistent with both the so-called partially disordered and the amplitude-modulated antiferromagnetic arrangements of the ferrimagnetic chains [27]. In this work, we focus only on the intrachain interactions, and do not address the question of interchain magnetic order.

In Fig. 2(a) we plot the energy-resolved density of states on the Ir ion, with the projections on the $|3z^2-r^2\rangle$ orbital plotted separately, from DFT+U+SOC calculations. In our choice of coordinate axes, shown in Fig. 1(b), the $|3z^2-r^2\rangle$ orbital of Ir has t_{2g}-like character with lobes extended towards the nearest neighbor Ni ions as shown in Fig. 1(c). This makes it the most important orbital for the superexchange interactions [28]. The Ir^{4+} cation has five d electrons in its valence shell. Its unoccupied e_g states lie between 3 and 4 eV (not shown), and it has a single Ir t_{2g} hole between 0.5 and 1.0 eV. This hole has 36% $|3z^2 - r^2\rangle$ character, and a nontrivial spin characteristic: its $|3z^2 - r^2\rangle$ contribution has the opposite spin relative to the rest of the hole, as seen in the energy-resolved spin expectation value $\langle S_z\rangle$ in Fig. 2(c). This can be explained by the strong SOC of the Ir ion: the hole on the Ir does not have a definite spin, but it has $J_{\text{eff}} = 1/2$ character and can be thought to have a corresponding *pseudo*spin. The $J_{\text{eff}} = 1/2$ orbitals with pseudospin in the $\mp\hat{z}$ directions are

$$|J_{1/2},\uparrow\rangle = \frac{1}{\sqrt{|\gamma|^2+2}}\left(i\gamma|A,\downarrow\rangle + \sqrt{2}|E^+,\uparrow\rangle\right) \qquad (1)$$

and

$$|J_{1/2},\downarrow\rangle = \frac{1}{\sqrt{|\gamma|^2+2}}\left(i\gamma|A,\uparrow\rangle + \sqrt{2}|E^-,\downarrow\rangle\right) \qquad (2)$$

where $|A\rangle = |3z^2 - r^2\rangle$ and $|E^{\mp}\rangle$ are the t_{2g}-like orbitals that are split by the trigonal field. (In the absence of the trigonal crystal field, $\gamma = 1$.) As a result, *the spin moment on the* $|A\rangle = |3z^2 - r^2\rangle$ *orbital is opposite to the total spin moment (as well as the pseudospin moment) of the Ir ion when it is along the z direction.*

Magnetic interactions — The effective magnetic Hamiltonian for the Ir ion with an electron in the $J_{\text{eff}} = 1/2$ orbital needs to be built using not the spin, but rather the pseudospin of the electron. The SOC reduces the orbital degeneracy in iridates, but the magnetic Hamiltonians are usually more complicated and may involve anisotropic exchange interactions which couple different components of pseudospins with different strengths [3, 29]. Anisotropic exchange interactions can set a preferred axis for the pseudospin moments and give rise to other effects that are usually ascribed to SIA. For example, the magnon gap observed in $Sr_3Ir_2O_7$ is explained by the exchange anisotropy between the Ir^{4+} ions [30].

The GKA rules [31] for the signs of the exchange interactions do not directly apply to the pseudospins since the orbital degree of freedom is entangled with spin [10]. Instead, we need to consider the individual orbital components of the $J_{\text{eff}} = 1/2$ spin-orbitals and the interactions between them. A tight binding model constructed using the ab-initio Wannier functions [32, 33] that only includes the Ni d and Ir t_{2g} orbitals shows that the largest hopping is between the $|A\rangle$ orbital on the Ir and the sim-

ilar $|3z^2 - r^2\rangle$ on the Ni as expected in this face-sharing polyhedral geometry [28].

The DOS projected onto Ni [28] shows that the $|3z^2 - r^2\rangle$ orbital on Ni^{2+} is fully occupied. The superexchange process in which a Ni electron is excited to an Ir $|A\rangle$ orbital is possible only if the electron has opposite spin to the spin on the Ir $|A\rangle$ orbital, and provides an energy gain proportional to the Ni on-site Hund's coupling if the Ni spin is parallel to that on the Ir $|A\rangle$ orbital [31]. This implies that there is a ferromagnetic coupling between the Ni spin and the spin on the Ir $|A\rangle$ orbital. Since the total spin expectation value $\langle S_z\rangle$ of the Ir ion is opposite to the spin on the Ir $|A\rangle$ orbital, this superexchange provides an antiferromagnetic (ferrimagnetic) coupling between the total magnetic moments of the Ni and the Ir ions. The inclusion of other orbitals in this argument [28] does not change the sign of this coupling, which explains the ferrimagnetic ground state observed in Sr_3NiIrO_6.

In our picture, then, this antiferromagnetic interaction, which emerges from a ferromagnetic superexchange, is a direct result of the strong SOC on the Ir ion. In order to test this claim further, we repeated a similar DFT calculation with SOC turned off, and could stabilize only the FM configuration. This is consistent with Ref. [24] where SOC was not taken into account and consequently only the FM order was stabilized. A similar point about different orbitals contributing to superexchange in a nontrivial way due to SOC is also made in Ref. 13, where a ferromagnetic exchange anisotropy stemming from an antiferromagnetic exchange interaction in Sr_3CuIrO_6 is studied.

Anisotropic exchange — The Ir $|A\rangle$ orbital has opposite spin to that of the $|E^{\mp}\rangle$ orbitals only when the Ir pseudospin is along $\hat{z}$. If the Ir magnetic moment is in another direction, this condition will no longer be satisfied. For example, the $J_{\rm eff} = 1/2$ state with pseudospin parallel to $\hat{x}$, $|J_{1/2}, \uparrow_x\rangle = \left(|J_{1/2}, \uparrow\rangle + |J_{1/2}, \downarrow\rangle\right)/\sqrt{2}$, has the form

$$|J_{1/2}, \uparrow_x\rangle = \Big(i\gamma\sqrt{2}|A, \uparrow_x\rangle + |E^+, \uparrow_x\rangle + |E^-, \uparrow_x\rangle + |E^+, \downarrow_x\rangle - |E^-, \downarrow_x\rangle\Big)/\sqrt{2(|\gamma|^2+2)} \quad (3)$$

where $|\uparrow_x\rangle = (|\uparrow\rangle + |\downarrow\rangle)/\sqrt{2}$ and $|\downarrow_x\rangle = (|\uparrow\rangle - |\downarrow\rangle)/\sqrt{2}$. The spin on the $|A\rangle$ orbital is now parallel to the pseudospin of the $|J_{\rm eff}, \uparrow_x\rangle$ orbital. DFT results with the spins aligned in the x-y plane, shown in Fig. 2(c) and (d), are consistent with this observation: the $\langle S_x\rangle$ of the hole on $|A\rangle$ is parallel to the minority spin direction. In this case, the ferromagnetic superexchange between the Ni ion and the Ir $|A\rangle$ orbital should give rise to a ferromagnetic coupling between the magnetic moments of these ions. In other words, the effective interaction between the magnetic moments M on the nearest-neighbor Ni-Ir atoms is anisotropic and has the form $E \sim J_{\parallel} M_z^{\rm Ir} M_z^{\rm Ni} + J_{\perp} M_{xy}^{\rm Ir} M_{xy}^{\rm Ni}$ with $J_{\parallel} > 0$ but $J_{\perp} < 0$.

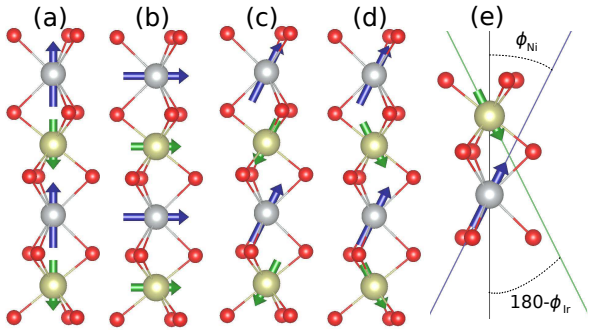

FIG. 3. (Color Online) (a) Ferrimagnetic state with moments along the z axis, which is the lowest-energy state (FiM-z: $\phi_{\rm Ni-Ir} = 180°$, $\phi_{\rm Ni} = 0°$, $\phi_{\rm Ir} = 180°$). (b) Ferromagnetic state with moments along the x axis (FM-x: $\phi_{\rm Ni-Ir} = 0°$, $\phi_{\rm Ni} = 90°$, $\phi_{\rm Ir} = 90°$). (c) Possible ferrimagnetic intermediate state ($\phi_{\rm Ni-Ir} = 180°$). (d) Observed, canted ferrimagnetic intermediate state ($\phi_{\rm Ni-Ir} < 180°$). (e) Definition of $\phi_{\rm Ni}$ and $\phi_{\rm Ir}$.

DFT calculations provide estimates of $J_{\perp}$ and $J_{\parallel}$ that support this claim. We adopt the standard approach of initiating the DFT calculations in different magnetic configurations to estimate the energy differences between various magnetic states. However, especially in non-collinear calculations, it is not always possible to stabilize the system in the desired local energy minima if the system is very far from its groundstate [34]. When we initiate our DFT calculation with spins parallel to $\hat{z}$, all of our calculations (even those initiated with FM order) converge to the ferrimagnetic configuration (FiM-z, Fig. 3(a)). On the other hand, we could not stabilize a FiM state with spins in the x-y plane; the only state we could stabilize with moments in the x-y plane is the ferromagnetic one (FM-x, Fig. 3(b)).

To gain information about the magnetic interactions, then, we compute the energy at both of the energy minima (FM-x and FiM-z, shown in Fig. 3(a) and (b)), where it is possible to converge the electronic state to a very high precision, and also at several intermediate states where the magnetic moments are tilted. We do not observe any local minima in the vicinity of these intermediate states, but the slope of the electronic energy surface is so small (changing by less than about 10^{-5} eV/atom from one self-consistent iteration to the next) that we believe it is well justified to estimate the energy of these intermediate states in this way [35].

We summarize our results in Fig. 4(a) and (b). The horizontal axis in these plots is the relative angle between the magnetic moments of Ir and Ni ions, $\phi_{\rm Ni-Ir}$. In Fig. 4(a) we plot the total energy per formula unit, and in Fig. 4(b), we plot the angles $\phi_{\rm Ir}$ and $\phi_{\rm Ni}$ that the two magnetic moments make with the z axis (as defined in Fig. 3(e)). There is a clear trend in $\phi_{\rm Ir}$ and $\phi_{\rm Ni}$ as a function of $\phi_{\rm Ni-Ir}$. The only ferromagnetic state ($\phi_{\rm Ni-Ir} = 0$) is observed when $\phi_{\rm Ir} = \phi_{\rm Ni} = 90°$, consistent with the

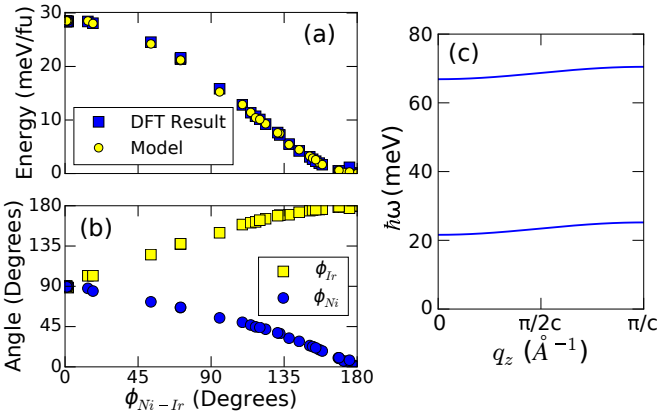

FIG. 4. (Color Online) First-principles results for the intra-chain magnetic interaction between Ni and Ir atoms. (a) Energy as a function of the angle between the magnetic moments of nearest-neighbor atoms. (b) The angle that the Ir and Ni magnetic moments make with the [001] axis as a function of the angle between the magnetic moments of nearest-neighbor atoms. (c) Magnon spectra of Sr_3NiIrO_6 along the [001] direction in the magnetically ordered phase.

previous observation that we could stabilize FM only if the moments are in the x-y plane (Fig. 3(b)). Similarly, ferrimagnetic order ($\phi_{\mathrm{Ni-Ir}} = 180°$) is observed only for $\phi_{\mathrm{Ir}} = 180°$ and $\phi_{\mathrm{Ni}} = 0°$, i.e., only when the moments are along $\mp\hat{z}$ (Fig. 3(a)). The intermediate data points in Fig. 4(a) and (b) correspond to intermediate states where the moments have their z components ordered ferrimagnetically while the x components are ordered ferromagnetically (Fig. 3(d)). Replacing the anisotropic with an isotropic Heisenberg interaction and instead using the SIA to explain the Ising behaviour would result in intermediate states with antialigned moments tilted away from the high symmetry axes, such as those shown in Fig. 3(c). However, we never observed an intermediate state like this in Sr_3NiIrO_6, supporting the view that the interactions between the Ni and Ir ions are strongly anisotropic.

Fitting the energy values to the anisotropic exchange model, we get $J_{\parallel} = 19.0\,\mathrm{meV}/\mu_B^2$ and $J_{\perp} = -8.4\,\mathrm{meV}/\mu_B^2$. This simple model fits the data quite well and gives the red data points in Fig. 4(a). The discrepancy between the first-principles results and the model is due to both the numerical error and a possible small SIA.

This is not the first study which uses an anisotropic exchange model for a compound with the K_4CdCl_6 structure. For example, Yin et al. have employed and microscopically justified a similar model to explain the magnetic anisotropy and magnon spectrum of Sr_3CuIrO_6 [13, 36]. Also, both Toth et al. [21] and Lefrancois et al. [20] used a similar model to explain their experimental observations of magnon spectra of Sr_3NiIrO_6. However, to the best of our knowledge, this is the first time that the exchange parameters $J_{\perp}$ and $J_{\parallel}$ are extracted from first principles and microscopically justified for this compound. This is also the first prediction of opposite signs for $J_{\perp}$ and $J_{\parallel}$. The connection between the magnetic anisotropy and exchange interactions were apparent in the results of Gordon et al. [26], who determined that the FM order is more stable when the spins are aligned in the x-y plane, but their approach focused on the spin, not the pseudospin, of the Ir ion, and did not permit the construction of a simple magnetic Hamiltonian.

We have intentionally refrained from introducing a SIA term into our model to emphasize that the physics of Sr_3NiIrO_6 can be explained without it. A large SIA term is not physically justified in this compound: in a cubic environment Ni^{2+} has two e_g holes, and therefore no orbital angular momentum, and the $J_{\mathrm{eff}} = 1/2$ states of Ir are SU(2) symmetric and therefore are not supposed to have any SIA. The trigonal crystal field necessarily breaks this simple picture, but there is no apparent reason why the trigonal field in this material should be strong enough to give rise to a record-breaking coercive field as well as a very large magnon gap. The anisotropic exchange interaction, on the other hand, leads to a magnetic anisotropy energy that is the same order of magnitude as the magnetic exchange itself, and can be used to explain the large observed coercive field.

Magnons — Magnons are commonly used to probe the nature of magnetic interactions. There are both inelastic neutron scattering (INS) and resonant inelastic X-ray scattering (RIXS) experiments that probed the magnon spectrum of Sr_3NiIrO_6 [20, 21]. Even though each method is sensitive to only one of the two magnon branches in this compound, together they present a coherent picture: One of the branches has a width of ∼10 meV, and is around ∼35 meV. The other branch, dominated by Ir, is at ∼90 meV, and is almost dispersionless. These observations of a large magnon splitting and gap, much larger than the bandwidth, have previously been explained by a combination of anisotropic exchange, SIA, and Dzyaloshinskii-Moriya interactions [20, 21]. Here we calculate the magnon spectrum of Sr_3NiIrO_6 using only the anisotropic exchange model with parameters from first principles to show that a model without SIA is sufficient to explain the large gap in the magnon spectrum.

We present the magnon spectra in Fig. 4(c) [28]. Our results correctly reproduce a large gap both between the two magnon branches, and between the lower branch and the zero-energy axis. The quantitative agreement is not perfect, but his can be possibly fixed by fine-tuning the U parameters.

The sign of $J_{\perp}$ does not enter into the energy expression for the magnons, so the magnon spectra do not provide any evidence for the sign difference between $J_{\parallel}$ and $J_{\perp}$. However, the relative intensities of the two branches carry information about this sign difference. While a precise calculation of the cross sections for an inelastic neutron scattering experiment is beyond the scope of this

study, in the supplemental information we provide a simple calculation that shows how the relative magnitudes of the magnon creation cross sections of the two bands depend on the sign and not just the magnitude of $J_\perp$. So far, the only neutron scattering study on this compound [21] could not observe the higher energy branch, and as a result there is no data to verify our prediction.

Conclusions — The magnetic exchange interaction between the nearest neighbor Ni-Ir ions is not an isotropic Heisenberg exchange, but is rather strongly anisotropic: The different components of magnetic moments are coupled with opposite signs. This explains both the Ising-type anisotropy and the large magnon gap without a large, physically unjustified SIA, thus resolving the mystery of the large coercivity observed. While magnon frequencies do not distinguish between competing models, we propose that measurements of relative magnon cross sections are capable of doing so.

This work was supported by NSF DMREF Grant DMR-1629059.

[1] William Witczak-Krempa, Gang Chen, Yong Baek Kim, and Leon Balents, "Correlated Quantum Phenomena in the Strong Spin-Orbit Regime," Annual Review of Condensed Matter Physics **5**, 57–82 (2014).

[2] Jeffrey G Rau, Eric Kin-Ho Lee, and Hae-Young Kee, "Spin-orbit physics giving rise to novel phases in correlated systems: Iridates and related materials," Annual Review of Condensed Matter Physics **7**, 195–221 (2016).

[3] Giniyat Khaliullin, "Orbital order and fluctuations in mott insulators," Progress of Theoretical Physics Supplement **160**, 155–202 (2005).

[4] Maria Hermanns, Itamar Kimchi, and Johannes Knolle, "Physics of the kitaev model: fractionalization, dynamical correlations, and material connections," arXiv preprint arXiv:1705.01740 (2017).

[5] Marjana Ležaić and Nicola A. Spaldin, "High-temperature multiferroicity and strong magnetocrystalline anisotropy in 3*d*-5*d* double perovskites," Phys. Rev. B **83**, 024410 (2011).

[6] K. Rolfs, S. Tóth, E. Pomjakushina, D. T. Adroja, D. Khalyavin, and K. Conder, "Incommensurate magnetic order in a quasicubic structure of the double-perovskite compound Sr_2NiIrO_6," Phys. Rev. B **95**, 140403 (2017).

[7] Onur Erten, O. Nganba Meetei, Anamitra Mukherjee, Mohit Randeria, Nandini Trivedi, and Patrick Woodward, "Theory of half-metallic ferrimagnetism in double perovskites," Phys. Rev. Lett. **107**, 257201 (2011).

[8] Ryan Morrow, Rohan Mishra, Oscar D Restrepo, Molly R Ball, Wolfgang Windl, Sabine Wurmehl, Ulrike Stockert, Bernd Buchner, and Patrick M Woodward, "Independent ordering of two interpenetrating magnetic sublattices in the double perovskite Sr_2CoOsO_6," Journal of the American Chemical Society **135**, 18824–18830 (2013).

[9] Hena Das, Prabuddha Sanyal, T. Saha-Dasgupta, and D. D. Sarma, "Origin of magnetism and trend in T_c in cr-based double perovskites: Interplay of two driving mechanisms," Phys. Rev. B **83**, 104418 (2011).

[10] Ryan Morrow, Kartik Samanta, Tanusri Saha Dasgupta, Jie Xiong, John W Freeland, Daniel Haskel, and Patrick M Woodward, "Magnetism in Ca_2CoOsO_6 and Ca_2NiOsO_6: Unraveling the mystery of superexchange interactions between 3d and 5d ions," Chemistry of Materials **28**, 3666–3675 (2016).

[11] Günter Bergerhoff and O Schmitz-Dumont, "Die kristallstruktur des kaliumhexachlorocadmats (ii)," Zeitschrift für anorganische und allgemeine Chemie **284**, 10–19 (1956).

[12] Hua Wu, T. Burnus, Z. Hu, C. Martin, A. Maignan, J. C. Cezar, A. Tanaka, N. B. Brookes, D. I. Khomskii, and L. H. Tjeng, "Ising magnetism and ferroelectricity in Ca_3CoMnO_6," Phys. Rev. Lett. **102**, 026404 (2009).

[13] Wei-Guo Yin, X. Liu, A. M. Tsvelik, M. P. M. Dean, M. H. Upton, Jungho Kim, D. Casa, A. Said, T. Gog, T. F. Qi, G. Cao, and J. P. Hill, "Ferromagnetic exchange anisotropy from antiferromagnetic superexchange in the mixed $3d-5d$ transition-metal compound Sr_3CuIrO_6," Phys. Rev. Lett. **111**, 057202 (2013).

[14] E. V. Sampathkumaran and Asad Niazi, "Superparamagnetic-like ac susceptibility behavior in the partially disordered antiferromagnetic compound Ca_3CoRhO_6," Phys. Rev. B **65**, 180401 (2002).

[15] S. Niitaka, K. Yoshimura, K. Kosuge, M. Nishi, and K. Kakurai, "Partially disordered antiferromagnetic phase in Ca_3CoRhO_6," Phys. Rev. Lett. **87**, 177202 (2001).

[16] D Mikhailova, CY Kuo, P Reichel, AA Tsirlin, A Efimenko, M Rotter, M Schmidt, Z Hu, TW Pi, LY Jang, *et al.*, "Structure, magnetism, and valence states of cobalt and platinum in quasi-one-dimensional oxides A_3CoPtO_6 with A= Ca, Sr," The Journal of Physical Chemistry C **118**, 5463–5469 (2014).

[17] TN Nguyen, DM Giaquinta, and H-C Zur Loye, "Synthesis of the new one-dimensional compound Sr_3NiPtO_6: Structure and magnetic properties," Chemistry of materials **6**, 1642–1646 (1994).

[18] TN Nguyen and H-C Zur Loye, "A family of one-dimensional oxides: Sr_3MIrO_6 (M= Ni, Cu, Zn): Structure and magnetic properties," Journal of Solid State Chemistry **117**, 300–308 (1995).

[19] John Singleton, Jae Wook Kim, Craig V. Topping, Anders Hansen, Eun-Deok Mun, S. Chikara, I. Lakis, Saman Ghannadzadeh, Paul Goddard, Xuan Luo, Yoon Seok Oh, Sang-Wook Cheong, and Vivien S. Zapf, "Magnetic properties of Sr_3NiIrO_6 and Sr_3CoIrO_6: Magnetic hysteresis with coercive fields of up to 55 t," Phys. Rev. B **94**, 224408 (2016).

[20] E. Lefrançois, A.-M. Pradipto, M. Moretti Sala, L. C. Chapon, V. Simonet, S. Picozzi, P. Lejay, S. Petit, and R. Ballou, "Anisotropic interactions opposing magnetocrystalline anisotropy in Sr_3NiIrO_6," Phys. Rev. B **93**, 224401 (2016).

[21] S. Toth, W. Wu, D. T. Adroja, S. Rayaprol, and E. V. Sampathkumaran, "Frustrated ising chains on the triangular lattice in Sr_3NiIrO_6," Phys. Rev. B **93**, 174422 (2016).

[22] Grigori V Vajenine, Roald Hoffmann, and Hans-Conrad zur Loye, "The electronic structures and magnetic properties of one-dimensional ABO_6 chains in Sr_3ABO_6 (A= Co, Ni; B= Pt, Ir) and two-dimensional MO_3 sheets in

$InMO_3$ (M= Fe, Mn)," Chemical physics **204**, 469–478 (1996).
[23] GR Zhang, XL Zhang, T Jia, Z Zeng, and HQ Lin, "Intrachain antiferromagnetic interaction and mott state induced by spin-orbit coupling in Sr_3NiIrO_6," Journal of Applied Physics **107**, 09E120 (2010).
[24] Soumyajit Sarkar, Sudipta Kanungo, and T. Saha-Dasgupta, "Ab initio study of low-dimensional quantum spin systems Sr_3NiPtO_6, Sr_3CuPtO_6, and Sr_3NiIrO_6," Phys. Rev. B **82**, 235122 (2010).
[25] Xuedong Ou and Hua Wu, "Impact of spin-orbit coupling on the magnetism of Sr_3MIrO_6 (M= Ni, Co)," Scientific reports **4** (2014).
[26] Elijah E Gordon, Hongjun Xiang, Jürgen Köhler, and Myung-Hwan Whangbo, "Spin orientations of the spin-half Ir^{4+} ions in Sr_3NiIrO_6, Sr_2IrO_4, and Na_2IrO_3: Density functional, perturbation theory, and madelung potential analyses," The Journal of chemical physics **144**, 114706 (2016).
[27] E. Lefrançois, L. C. Chapon, V. Simonet, P. Lejay, D. Khalyavin, S. Rayaprol, E. V. Sampathkumaran, R. Ballou, and D. T. Adroja, "Magnetic order in the frustrated ising-like chain compound Sr_3NiIrO_6," Phys. Rev. B **90**, 014408 (2014).
[28] See the supplemental information for details.
[29] G. Jackeli and G. Khaliullin, "Mott insulators in the strong spin-orbit coupling limit: From heisenberg to a quantum compass and kitaev models," Phys. Rev. Lett. **102**, 017205 (2009).
[30] Jungho Kim, A. H. Said, D. Casa, M. H. Upton, T. Gog, M. Daghofer, G. Jackeli, J. van den Brink, G. Khaliullin, and B. J. Kim, "Large spin-wave energy gap in the bilayer iridate $Sr_3Ir_2O_7$: Evidence for enhanced dipolar interactions near the mott metal-insulator transition," Phys. Rev. Lett. **109**, 157402 (2012).
[31] J.B. Goodenough, *Magnetism and the chemical bond*, Interscience monographs on chemistry: Inorganic chemistry section (Interscience Publishers, 1963).
[32] Nicola Marzari, Arash A. Mostofi, Jonathan R. Yates, Ivo Souza, and David Vanderbilt, "Maximally localized wannier functions: Theory and applications," Rev. Mod. Phys. **84**, 1419–1475 (2012).
[33] Nicola Marzari and David Vanderbilt, "Maximally localized generalized wannier functions for composite energy bands," Phys. Rev. B **56**, 12847–12865 (1997).
[34] Some other studies (Refs. 23 and 25) found similar behavior.
[35] Keeping the calculation running until selfconsistency results in these intermediate states eventually converging to either FM-x or FiM-z.
[36] X Liu, Vamshi M Katukuri, L Hozoi, Wei-Guo Yin, MPM Dean, MH Upton, Jungho Kim, D Casa, A Said, T Gog, *et al.*, "Testing the validity of the strong spin-orbit-coupling limit for octahedrally coordinated iridate compounds in a model system Sr_3CuIrO_6," Physical review letters **109**, 157401 (2012).